Acoustic Signature Measurement to Identify Laser-Induced Breakdown in Water during Laser Shock Peening

Marek Böhm[1,2], Josef Blažej[2], Ondřej Stránský[1,3], Jan Kaufman[1], Jan Brajer[1,3], Sunil Pathak[*1,3,4], and Tomáš Mocek[1]

[1]*HiLASE Centre, Institute of Physics of the Czech Academy of Sciences, Za Radnicí 828, Dolní Břežany, 25241, Czech Republic.*
[2]*Faculty of Nuclear Sciences and Physical Engineering, Czech Technical University in Prague, Trojanova 339, Prague, 12000, Czech Republic.*
[3]*Faculty of Mechanical Engineering, Czech Technical University in Prague, Technická 4, Prague, 16000, Czech Republic.*
[4]*School of Smart Manufacturing, New Age Makers Institute of Technology, Gandhinagar Gujarat, India*
**Corresponding author's. E-mails: sunil.pathak@hilase.cz, sunilpathak87@gmail.com*

A prevalent non-destructive evaluation method for identifying and analyzing the acoustic waves produced by material deformation and damage is acoustic emission monitoring. In this work, laser shock peening was used in conjunction with acoustic emission monitoring. To determine the acoustic event of laser-induced breakdown in water, the acoustic signals were analyzed. To attain the required compressive residual stresses and prevent undesirable damage, the acoustic emission signals can also be utilized to optimize the laser shock peening parameters, such as the laser energy and spot size. Thus, to investigate the possibilities of acoustic emission monitoring as a tool for the in-situ characterization of laser shock peening, offering insights into the underlying physical processes and help improving the quality of the treated parts. It was found that the plasma breakdown during the laser shock peening intensely hinders the performance as a compressive residual stress on the surface were observed halved (from –216 MPa to –82 MPa) when comparing the setups with and without the plasma breakdown. Thus, by utilizing the acoustic signals the harmful laser-induced breakdown can be detected and optimizing it can enhance process efficacy.

DOI: 10.2961/ilmn.2025.02.2007
Keywords: laser shock peening, acoustic emission measurement, optical microphone, laser-induced breakdown

1. Introduction

Laser shock peening (LSP) is a surface engineering method that improves the fatigue life of metallic components. Increased yield strength of metallic materials is associated with the formation of high-density dislocation arrays and induced compressive residual stresses produced by LSP [1-3]. The potential for employing focused, high-energy laser pulses to generate high-pressure shock waves in metallic materials was identified in the United States [4]. LSP involves focusing a strong pulsed laser shock beam onto a metal surface for a short period of time (10 ns to 100 ns) [5-6]. Ionization converts the heated zone to plasma, which has a temperature of over 10 000 °C. Plasma is under high pressure and travels through the material by shock waves (Fig. 1) [7]. There are two distinct forms of ablation in LSP: confined ablation and direct ablation. The interaction of plasma with metal without an opaque covering and an optically transparent confinement layer is referred to as the "direct ablation mode" [8]. It is possible to generate plasma pressures sufficient to overcome the materials Hugoniot elastic limit (HEL) and thus induce plastic deformation during the direct ablation mode in vacuum. However, these necessitate extensive laser intensities. Instead, during the confinement mode e.g. when focusing the laser on the metallic surface with an optically transparent layer covering and confining the plasma, the efficiency of the process and the generated pressures are larger by a factor up to ten, but also increases the duration of plasma by a factor of three in comparison with the direct ablation mode such that the pressures in ranges of several GPa can be obtained without the need for vacuum. Past studies have established that the choice of confinement medium is central to the efficiency of LSP, with water and glass confinement being the most widely used approaches because they can maximize pressure transmission [2, 9]. It is well known that the confined ablation mode does more than just raise the plasma's peak pressure. In the confined mode, the metal surface is typically covered with an opaque material, such aluminum foil, black paint, or black tape, and enclosed by a material that is transparent to laser light, like borosilicate glass or water. At a deeper depth, compressive residual stresses are larger when the pressure wave is stronger [9]. It has been discovered that LSP performed in water confinement regime (WCR) can generate pressures on the target surface that are four times greater and last 2-3 times longer than those produced by direct ablation regime configurations in vacuum. The primary disadvantage of the WCR is that laser-induced breakdown occurs in water when the laser power density exceeds a certain threshold [10]. Laser-induced breakdown in confinement water refers to the creation of plasma (also called secondary or breakdown plasma) away from the material's surface, which then captures the incoming laser pulse and restricts the energy needed to create a shock wave [11]. This breakdown plasma partially or entirely blocks the incident laser pulse, and this plasma leads to the observed saturation of pressure during LSP.

Peak pressure measurements taken with three harmonics of the Nd:YAG laser indicate that pressure saturation happens at lower irradiance thresholds for 532 nm and 355 nm than at 1064 nm, suggesting that shorter wavelengths facilitate the breakdown process. Shifting the wavelength from 1064 nm to 532 nm decreases the threshold for dielectric breakdown from 10 GW/cm^2 to 6 GW/cm^2 [12].

At 1064 nm, avalanche ionization primarily governs the breakdown process, while at shorter wavelengths, multiphoton ionization becomes more dominant [11]. The laser pulse that passes through the breakdown plasma corresponds to the portion of the incident laser pulse that precedes the transmission cut-off [13]. A cavitation bubble is formed in the confinement water after laser ablation. Takata et al. extensively studied bubble formation, expansion and collapse with both high-speed camera and acoustic sensors. During intentionally generated laser-induced breakdown, the generation of a secondary bubble after the first one was discovered. This secondary bubble was generated by breakdown [15]. These effects are accompanied by acoustic emissions, and it is possible to distinguish sounds when a significant breakdown occurs. Kaleris et. al. [16, 17] has studied Laser-plasma sound sources in atmospheric air and has found that for increased optical energy there is a shift of the acoustic frequency spectrum towards the lower frequencies. Laser-plasma sound sources produce a characteristic N-pulse shape in the time domain. Increased optical energy leads to a longer duration of the thermal phase, which results in a wider N-pulse in the time domain. The wider N-pulse causes the shift of the acoustic spectrum towards the lower frequencies. Setup B with the breakdown in air can be considered an increase in optical energy thereby explaining the frequency shift to sub 1x10^4 Hz frequencies.

The LSP process is usually controlled post situ through the measurement of residual stresses introduced to the treated material. Such methods can be either non-destructive (X-ray diffraction, neutron diffraction etc.) or destructive (incremental hole drilling). Practically, it is not possible to carry out full and destructive testing on all treated specimens in the industrial setting therefore the need for in-situ, non-destructive quality control methods must be explored. Even with the well-documented advantages of LSP, a lack of real-time monitoring methodologies hinders industrial use. Integration of acoustic emission methods with LSP has been proposed as a means of achieving real-time process control, lessening dependency on post-processing assessment [23-24]. In the present an attempt has been made to explore the potential of acoustic emission monitoring as a tool for the in-situ characterization of LSP, providing insights into the underlying physical mechanism and helping to improve the quality and reliability of the treated materials. The experiments have been planned to see the effects of laser induced breakdown on the residual stresses generated in LSP treated sample and at the same time capturing the acoustic emission signals to understand the underlying effects.

2. Materials and Methods

Traditionally manufactured Aluminium AA2024 plate of dimension 100 × 100 × 5 mm was used for the present experiment. A pulsed Q-switched Nd:YAG laser Litron LPY ST 7875-10 2HG was used as a source for LSP processing of the samples. The parameters of this system are summarized for reference (Table 1 [15]). The experiments were performed without coating underwater and for this a second harmonic wavelength at 532 nm was used, the temperature of the water was set at 18 °C. The laser beam passed through a vacuumed telescope and was redirected by dual-band laser mirrors with anti-reflective coating. A rectangular pattern of overlapping (50%) pulse impacts was created by building the pattern line by line (Fig. 1). The experiments were performed using two arrangements for the LSP operation namely setup A and setup B. In setup A, the conventional LSP processing at known parameters to develop compressive residual stresses in AA2024 was used, while setup B used the same parameters, but the sample was moved farther away from the focusing lens, and laser-induced breakdown was deliberately created by concentrating a laser beam into the water. The parameters for the present experiments were selected based on the trial experiments and prior testing (Table 1).

The Setup was accompanied with diagnostics - energy meter, near field and far field camera, and photodiode. The beam was focused onto the sample using a plano-convex lens with a 300 mm focal length mounted on one side of an acrylic tank. The sample was positioned using a FANUC M-20iB/35B 6-axis industrial robotic arm. The profile of the laser pulse at 36 mJ recorded by an Allied Vision Manta G-210B ASG GigE near field camera is circular as shown in Fig. 3a. The temporal shape of the laser pulse measured by an InGaAs EOT ET-3000EXT PIN detector has a rise time of 7.2 ns (Fig. 2b).

Figure 3 presents a detailed schematic of the LSP experimental setup, it can be noticed from Fig. 3 that a Xarion Eta250 Ultra optical microphone is placed to record the acoustic signal emitted during the LSP process. The microphone head was kept at a constant distance of 36.5 cm from the sample. It consists of a miniaturized Fabry-Pérot laser interferometer (FPI) which allows to measure the changes in the density of the optical medium directly. The optical microphone consists of two units (a) the acoustic detection system, consisting of the optical sensor head and the driver unit comprising laser and detector and (b) an analogue-to-digital converter with acquisition software [18].

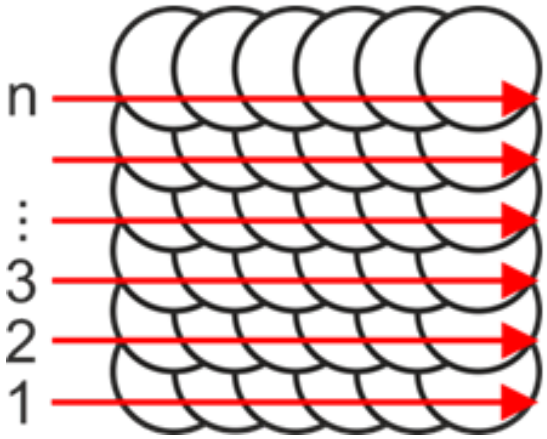

Fig. 1 Laser shock peening pattern creation methodology.

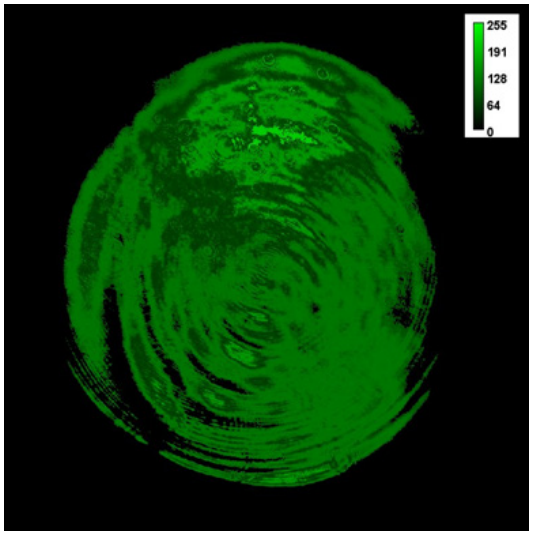

(a)

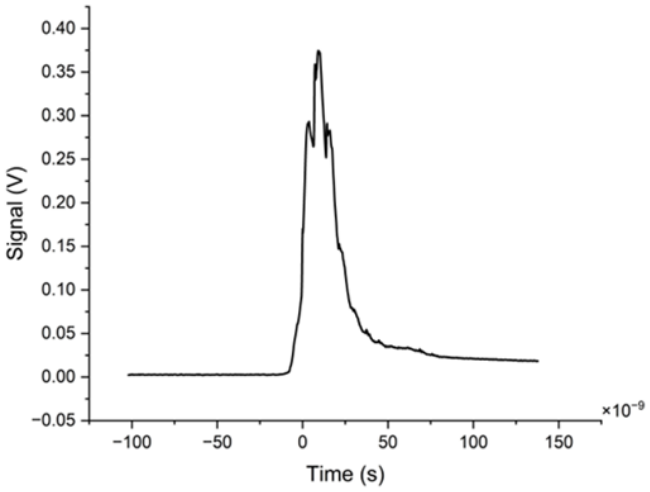

(b)

Fig. 2 (a) Near field camera profile of LPY ST 7875-10 2HG laser pulse; (b) Temporal shape of LPY ST 7875-10 2HG laser pulse.

Table 1 LSP processing parameters

Setup	A	B
Repetition Rate [Hz]	10	10
Distance from lens [m]	0.405	0.425
Pulse energy [mJ]	800	800
FWHM laser pulse [ns]	15.6	15.6
Dimple diameter [mm]	1.674	1.549
Overlap [%]	50	50
Power density I_0[GW/cm^2]	2.33	2.72

To measure the depth profile of the residual stresses an automated drilling and data collection system system PRISM by Stresstech was used to gain depth-resolved residual stress profiles. The hole drilling method is based on the measurements of surface distortion caused by drilling using electronic speckle pattern interferometry. For the measurement, the drill diameter of 3.2 mm was selected, enabling measurements up to 1.5 mm in depth. A series of 5 stress profiles per each condition was measured and averaged. Surface deformation measurement was carried out using a Keyence VR-6000 3D profilometer with a resolution of 0.1 µm. The measurement is contactless and works on the principle of fringe projection. The area of 5.5x7.5 mm was scanned on 40x magnification and evaluated in VR-6000 Series Analyzer Software version 4.3.7.74. To analyze the data generated from the signal captured by the optical microphone Mask testing has been utilized which is commonly used in signal processing to determine if a signal falls within predetermined tolerance boundaries, offering a straightforward pass/fail assessment to gauge the quality and stability of a device/process being tested. Deviations from expected signals and unforeseen outcomes are readily detected by halting the measurement when the signal exceeds the mask's limits. The captured acoustic signals underwent post-processing through Matlab software. The acoustic signals from Setup A and B were averaged from 100 recordings, and the averaged signal for Setups A and B from the time domain was converted into the frequency domain through the application of the Fast Fourier Transform (FFT). The maximum frequency was limited to 50 kHz. A mask was applied to the averaged signal. Mask testing enabled to observe the differences between acoustic signals temporal evolution of Setup A (before laser-induced breakdown) and Setup B (after laser-induced breakdown).

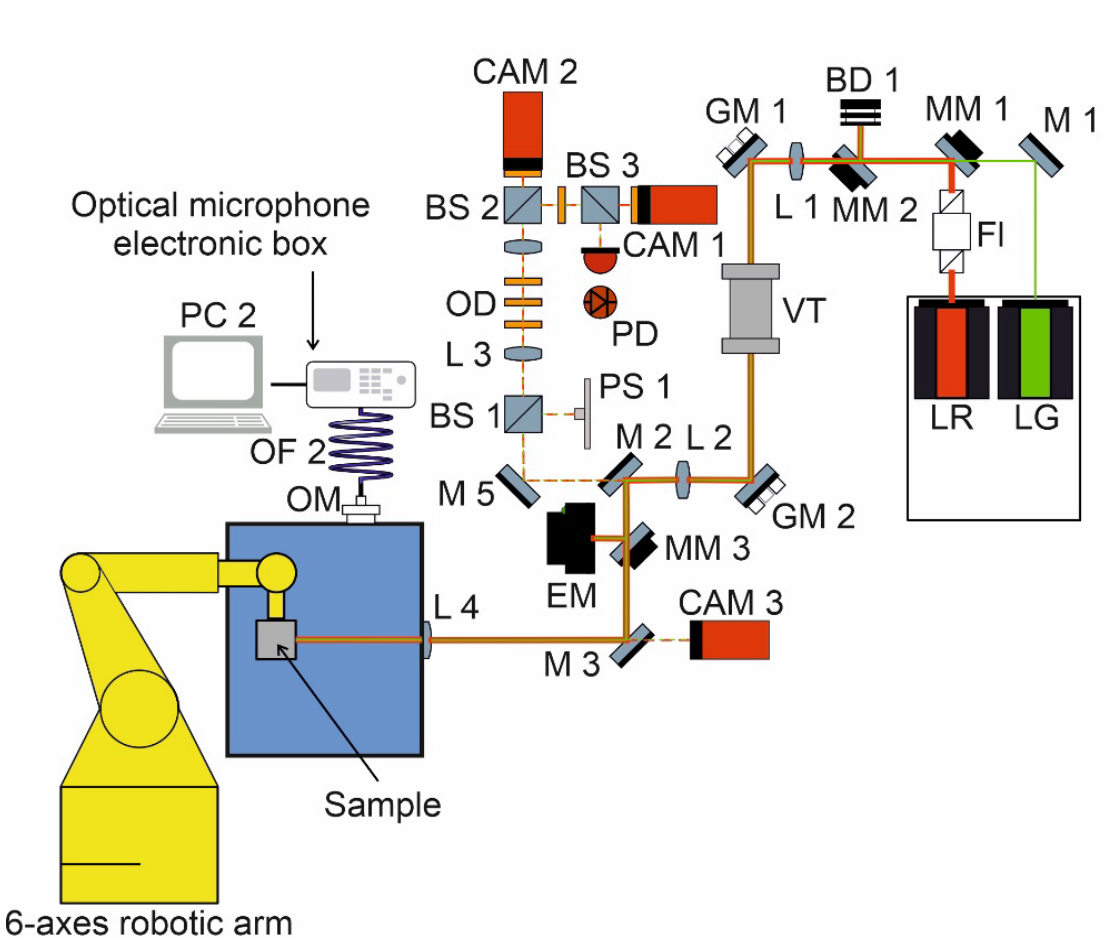

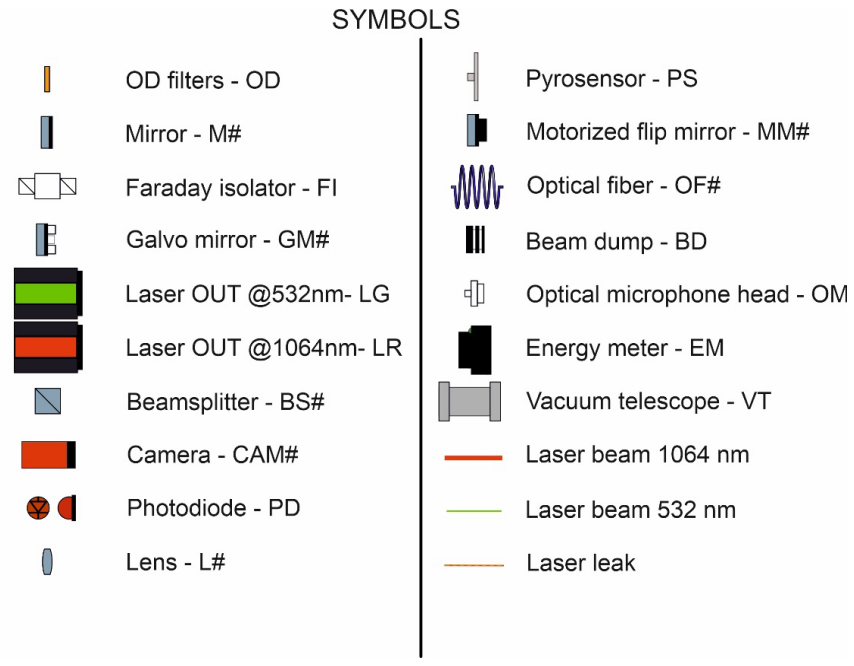

Fig. 3 Laser shock peening experimental Setup schematics.

3. Results and Discussion

The details of the residual stresses in the AA2024 material before LSP and after LSP utilizing the setup A and setup B, are presented in Fig. 4(a). It can be seen that Setup A (before laser-induced breakdown) parameters have enabled higher compressive residual stresses (i.e. −216 MPa) as compared to Setup B (after laser-induced breakdown) parameters (i.e. −82 MPa) near the peening surface region. Also, it can be observed that the penetration depth of residual stresses is higher in setup A (0.6 mm) compared to setup B (0.4 mm). The results of residual stress measurement fall within the expectation of the breakdown plasma occurring in water shielding the desired plasma forming on the sample surface, decreasing the laser intensity on the sample surface, thus reducing the pressure and, subsequently the whole efficiency of the LSP processing. Further, the obtained results can be justified with the help of FFT signals derived from the temporal acoustic signals for Setups A and B as presented in Fig, 4(b). It is known that the existence of plasma breakdown causes a distinct acoustic response in LSP processing [19]. In context of LSP, the correlation between acoustic emission (AE) and residual stress as the main outcome of the technology is being explored. The shift in AE signal characteristics – particularly frequency peaks serve as indicators for residual stress quality. By comparing the acoustic spectra of the two configurations, the difference in produced acoustic emission may be detected primarily below 2.5x10^4 Hz, as shown in Fig. 4(a). It can be noticed that in setup A, where the laser induced plasma breakdown does not play a role, the maximum available plasma is confined an transmitted in the form of pressure shock waves within the material and causes severe plastic deformation, which in turn generated higher magnitude of residual stresses at much deeper depth (Fig. 4a), at the same time it also generated a higher magnitude of peak 1.1x10^4 Hz. In setup A the main source of acoustic emission is the LSP induced plasma expansion and its subsequent collapse. In contrast, the plasma breakdown occurrence in water (as in Setup B) caused by the dielectric breakdown serves as a second source of acoustic emission away from the sample surface. The laser pulse is focused and propagates through the water medium. When a sufficient power density is reached the dielectric breaks down and the laser pulse loses significant portion of energy before reaching the sample. In this setup the acoustic emission occurs both on the sample surface and away from the surface, in the location of dielectric breakdown where a bubble is formed and quickly collapses. The energy reaching the sample surface is effectively lessened, lowering the maximum peak pressure of LSP which reflects in lower magnitude and depth of residual stresses. The produced sound in this configuration has higher magnitudes in lower frequencies with four distinctive peaks below the 1x10^4 Hz. In combination with different natural attenuations of the two compared setups, the frequency shift becomes more pronounced, and the difference can be found in the emission spectra as shown in Fig. 4b. Key frequency peaks are annotated in Fig. 4b. and their centres and amplitudes are listed in Table 2.

3.1 Surface deformation measurement

Type A parameters showed greater depth of single-shot impact deformation than Type B parameters (Fig. 5 and Fig. 6). The depth of the spot can be referred to the amount of residual stress introduced by LSP when comparing dimples processed on the same setup [20]. A change in the shape of the dimple was also observed, which can be attributed to different plasma mechanics and shielding of the sample surface by the plasma induced in the confining media. The reduced pressure on the sample surface in Setup B can overcome the HEL within a smaller area and with a lower magnitude; therefore, the shape of the dimple is altered. The dimple profile becomes sharper and reaches a lower depth.

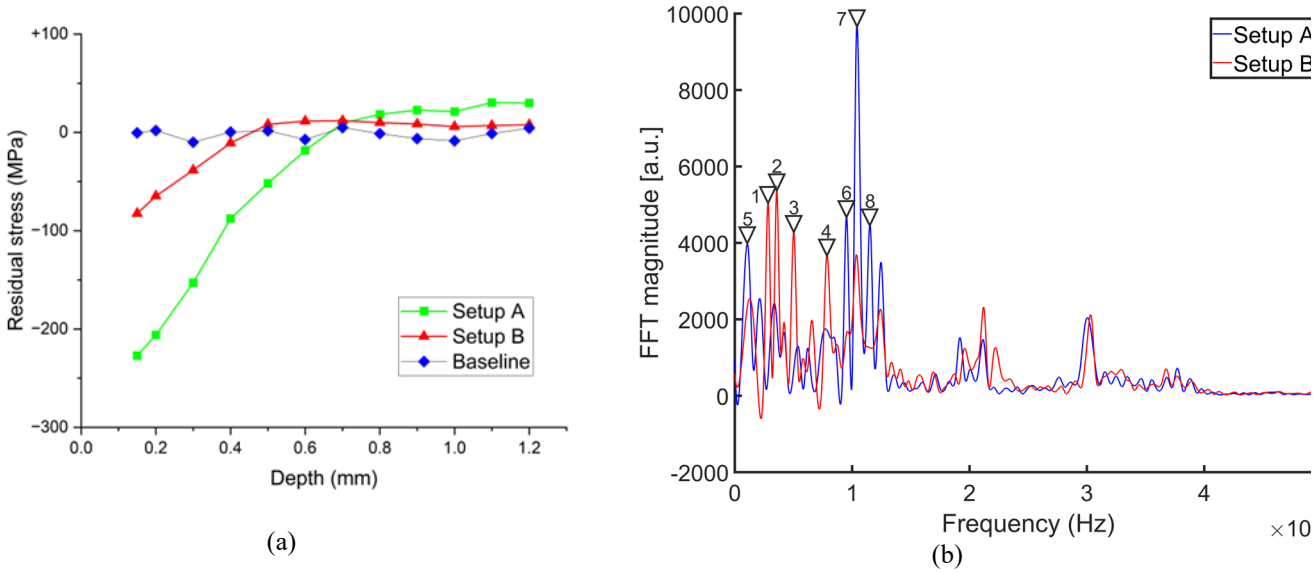

Fig. 4 (a) Incremental hole drilling depth residual stress; and (b) FFT derived from the temporal acoustic signals for Setups A and B.

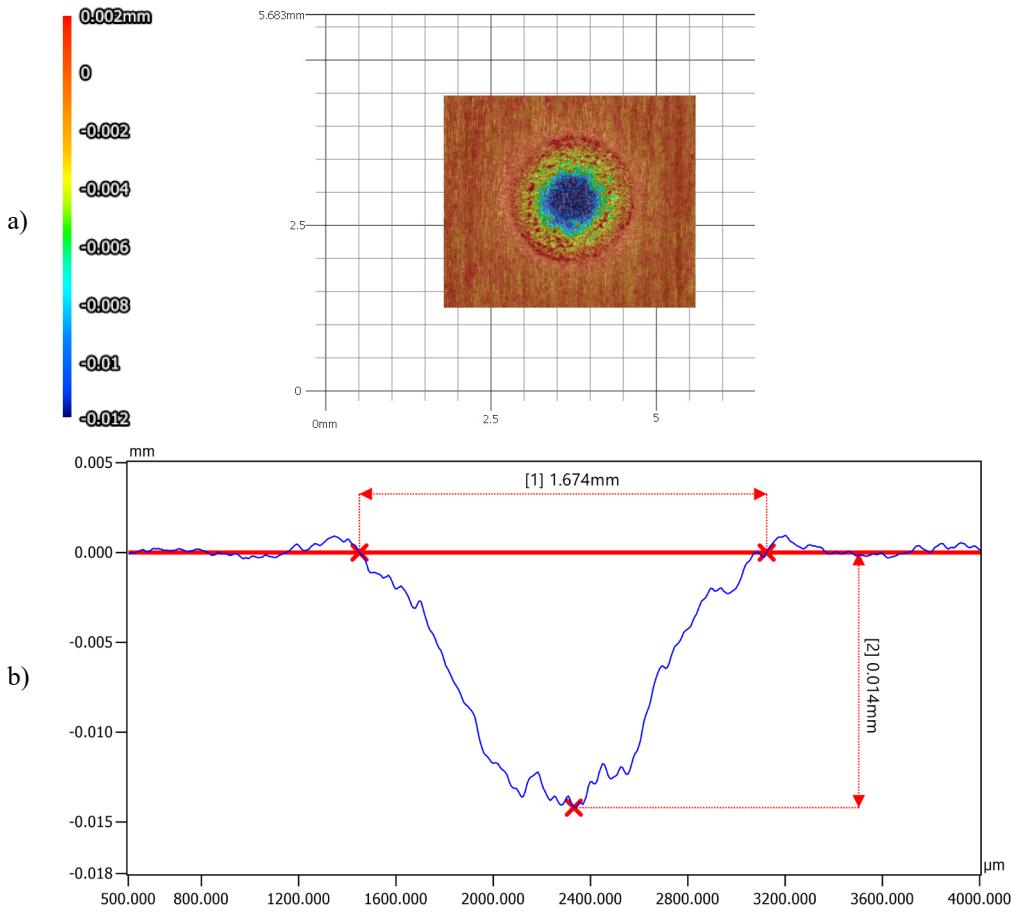

Fig. 5 Single laser shock impact Setup A: a) 3D data of the dimple, b) extracted profile.

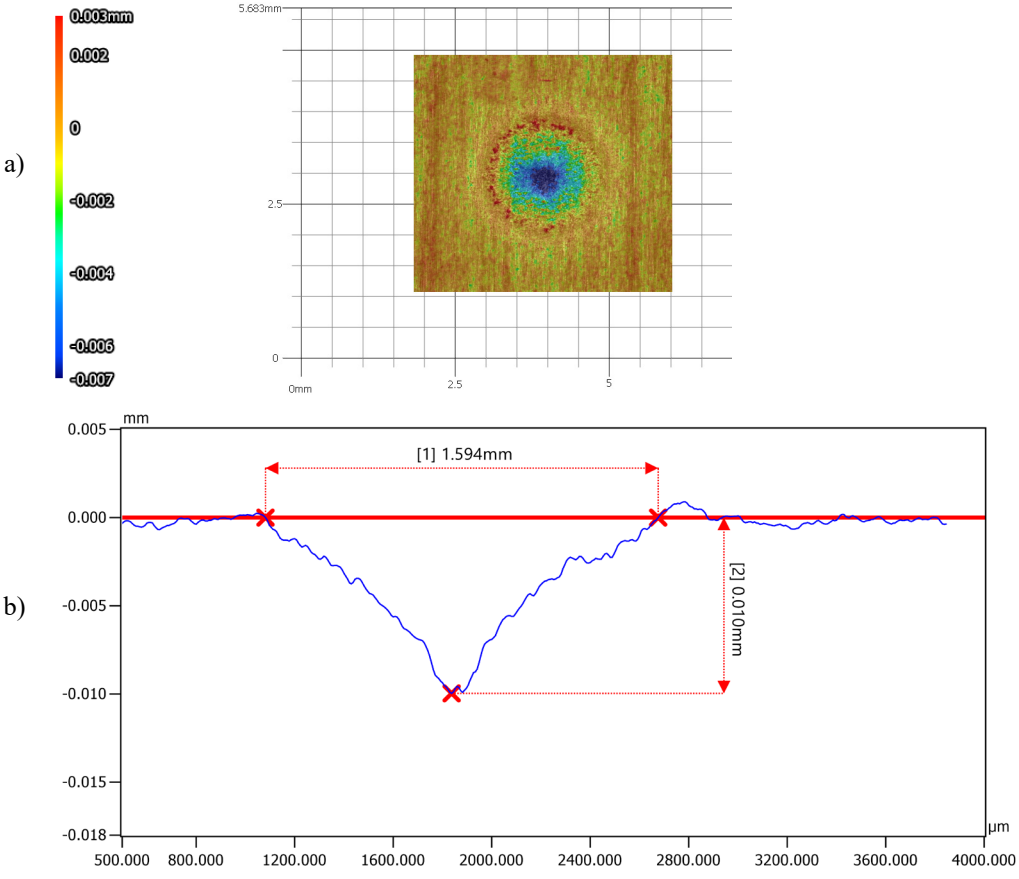

Fig. 6 Single laser shock impact Setup B: a) 3D data of the dimple, b) extracted profile.

Table 2 Selected peak positions and magnitudes marked in Figure 4b

Peak No.	Center [Hz]	Magnitude[a.u.]
Setup B		
1	2870	4972.49
2	3570	5388.64
3	5040	4282.37
4	7820	3640.30
Setup A		
5	1210	3573.07
6	9520	4702.12
7	10340	9205.54
8	11550	4460.24

4. Conclusions

This research shows the importance of in-situ quality control of the LSP process and its feasibility through acoustic emission. The results of the two setups with and without plasma breakdown occurrence were compared through the residual stress measurement on the surface and in depth, surface deformation and the acoustic emission spectra. The following conclusions can be attained:

1. Plasma breakdown occurrence was successfully induced by changes in LSP setup in controllable manner, thus the acoustic emission spectra can be compared.
2. It was noticed that the acoustic emission spectra of the two setups differ significantly therefore the in-situ detection of the plasma breakdown during the LSP process is possible allowing for fast and straightforward quality control.
3. By analysing the residual stresses induced by the two setups, it was noticed that the plasma breakdown during the LSP process strikingly hinders the performance of the LSP as a compressive residual stress inducing mechanism. The stresses on the surface were effectively halved (from –216 MPa to –82 MPa) when comparing the setups with and without the plasma breakdown. Similar findings can be deduced from the RS depth profiles where the A setup reached larger depth as well as contributed to roughly twice the magnitude of the compressive stress induced.
4. The plasma breakdown during the LSP processing alters not just the effectiveness of the processing in terms of residual stress but also reshapes the depth and the shape of the induced dimple. The reduction of depth of the dimple was observed from 0.014 mm to 0.010 mm.

Acknowledgement: This work was co-funded by European Union and the state budget of the Czech Republic under the project LasApp CZ.02.01.01/00/22_008/0004573.

Conflict of interest

Authors declare there is no conflict of interest.

References

[1] S. Pathak, M. Böhm, J. Kaufman, J. Kopeček, S. Zulić, O. Stránský, J. Brajer, L. Beránek, and T. Mocek: Surf. Eng., 39, (2023) 229.
[2] O. Stránský, S. Pathak, J. Kaufman, M. Böhm, J. Kopeček, L. Beránek, F. Holešovský, Š. Petrášek, L. Hlavůňková, and Z. Soukup: J. Mater. Res. Technol., (2023) 1683.
[3] J. Kaufman, J. Racek, M. Cieslar, P. Minárik, M. A. Steiner, S. R. Mannava, V. K. Vasudevan, A. Sharma, M. Böhm, J. Brajer, J. Pilař, L. Pína, and T. Mocek: Corros. Sci., 194, (2022) 109925.
[4] R. M. White: J. Appl. Phys., 34, (1963) 2123.
[5] S. Pathak, S. Zulić, J. Kaufman, J. Kopeček, O. Stránský, M. Böhm, J. Brajer, L. Beránek, A. Shukla, M. Ackermann, F. Véle, and T. Mocek: J. Mater. Res. Technol., 19, (2022) 4787.
[6] O. Stránský, I. Tarant, L. Beránek, F. Holešovský, S. Pathak, J. Brajer, T. Mocek, and O. Denk: Surf. Eng., 40, (2024) 66.
[7] R. Fabbro, P. Peyre, L. Berthe, and X. Scherpereel: J. Laser Appl., 10, (1998) 265.
[8] K. Ding and L. Ye: Laser Shock Peening, 1st ed., Woodhead Publ., Cambridge, (2006), p. 1.
[9] B. P. Fairand, A. H. Clauer, R. G. Jung, and B. A. Wilcox: Appl. Phys. Lett., 25, (1974) 431.
[10] R. Fabbro, J. Fournier, P. Ballard, D. Devaux, and J. Virmont: J. Appl. Phys., 68, (1990) 775.
[11] A. Sollier, L. Berthe, and R. Fabbro: Eur. Phys. J. Appl. Phys., 16, (2001) 131.
[12] L. Berthe, R. Fabbro, P. Peyre, L. Tollier, and E. Bartnicki: J. Appl. Phys., 82, (1997) 2826.
[13] L. Berthe, R. Fabbro, P. Peyre, and E. Bartnicki: Eur. Phys. J. Appl. Phys., 3, (1998) 215.
[14] T. Takata, M. Enoki, P. Chivavibul, A. Matsui, and Y. Kobayashi: Mater. Trans., 57, (2016) 674.
[15] Litron LPY Series High and Ultra-High Energy Q-Switched Nd:YAG Lasers. (2020). https://litron.co.uk/wp-content/uploads/2020/11/LPY-Series-November-2020.pdf
[16] K. Kaleris, Y. Orphanos , M. Bakarezos, V. Dimitriou ,M. Tatarakis, and J. Mourjopoulos: J. Phys. D: Appl. Phys., 53, (2020) 435207.
[17] K. Kaleris, Y. Orphanos, S. Petrakis, M. Bakarezos, M. Tatarakis, J. Mourjopoulos, and N. A. Papadogiannis: J. Sound Vib., 570, (2024) 118000.
[18] B. Fischer, W. Rohringer, N. Panzer, and S. Hecker: Laser Appl. Technol. J., (2017) 21.
[19] W. Wu, S. Chai, and Y. Zhou: Appl. Opt., 62, (2023) 9375.
[20] M. Dorman, M. B. Toparli, N. Smyth, A. Cini, M. E. Fitzpatrick, and P. E. Irving: Mater. Sci. Eng. A, 548, (2012) 142.

(Received: December 4, 2024, Accepted: June 29, 2025)